Advancement in screen printed fire through silver paste metallisation of polysilicon based passivating contacts

Chaudhary, Aditya; Hoß, Jan; Lossen, Jan; van Swaaij, René; Zeman, Miro

DOI
10.1063/5.0055978

Publication date
2021

Document Version
Final published version

Published in
Proceedings of the 9th Workshop on Metallization and Interconnection for Crystalline Silicon Solar Cells

Advancement in screen printed fire through silver paste metallisation of polysilicon based passivating contacts

Cite as: AIP Conference Proceedings **2367**, 020003 (2021); https://doi.org/10.1063/5.0055978
Published Online: 01 June 2021

Aditya Chaudhary, Jan Hoß, Jan Lossen, et al.

Advancement in Screen Printed Fire through Silver Paste Metallisation of Polysilicon Based Passivating Contacts

Aditya Chaudhary[1, 2, a)], Jan Hoß[1)], Jan Lossen[1)], René van Swaaij[2)], and Miro Zeman[2)]

[1]*International Solar Energy Research Center (ISC) Konstanz, Rudolf-Diesel-Str. 15, D-78467 Konstanz, Germany*
Phone: +49 7531 3618348; Fax: +49 7531 3618311

[2]*Delft University of Technology, Mekelweg 4, 2628 CD Delft, Netherlands*

[a)] *Corresponding author: aditya.chaudhary@isc-konstanz.de*

Abstract. We have metallised n+ polysilicon passivated layer structures deposited by Low Pressure Chemical Vapor Deposition (LPCVD) with silver pastes. We analysed recombination at the metal contacts by photoluminescence imaging of metallised lifetime samples and found for the best paste, metal semiconductor recombination current density values (J_{0met}) below 70 fA/cm^2, with contact resistivity below 2 mΩcm^2. To our knowledge, these are among the lowest values reported so far for full size M2 wafers with 150 nm thin polysilicon layer and wet chemical thin oxide. We also studied the effect of the peak firing temperature on the J_{0met} and contact resistivity in this work. Further, we performed Scanning Electron Microscopy to further understand the silver polysilicon interface.

INTRODUCTION

Passivated contacts based on polysilicon and a thin silicon oxide are currently one of the most researched topic in crystalline silicon photovoltaics with the potential to be the next evolutionary step after Passivated Emitter Rear Contact (PERC) cells. This is because of the various advantages associated to this concept of passivation. It has a high efficiency potential and it is suitable for the conventional high temperature process involved in crystalline silicon solar cell manufacturing, hence it can be adopted in an effective manner in existing solar-cell production lines [1].

Industrial TOPCon (Tunnel Oxide Passivated Contact) cells based on a rear polysilicon layer stacks are currently limited by the short-circuit current density (J_{sc}) [2, 3]. One of the reasons for a relatively low J_{sc} is parasitic absorption in the polysilicon layer used [1, 4, 5]. To reduce these losses, the plausible way is to reduce the polysilicon layer thickness. However, the thin polysilicon layer should still provide high level of passivation and a good contact (e.g. a low metal polysilicon recombination current density (J_{0met}) and low contact resistivity (ρ_c)) when metallised. For this purpose dedicated silver pastes have been developed by paste suppliers.

In this work, we use three different fire-through silver pastes (referred to as Paste A, B and C) that have been specially tailored for polysilicon contacting purposes and investigate the effect of the fast-firing peak temperature on J_{0met} and ρ_c for an n^+ polysilicon layer of 150 nm thickness. With our experiments, we provide insight into the performance of these pastes and demonstrate potential for metallising thinner polysilicon layers with the best paste.

EXPERIMENTAL

We made symmetrical lifetime samples by Low Pressure Chemical Vapor Deposition (LPCVD) at about 600 °C of approximately 150 nm n^+ doped polysilicon layer on top of ~ 1.4 nm thin silicon oxide layer on n-type CZ silicon wafers of ~ 180 µm thickness and a base resistivity of ~ 0.91 Ωcm. The polysilicon layer was subsequently annealed at a temperature of 825 °C for 30 minutes. Afterwards, ~ 80 nm of silicon nitride was deposited by PECVD on both sides of the samples. A schematic of the sample is shown in Fig. 1.

Proceedings of the 9th Workshop on Metallization and Interconnection for Crystalline Silicon Solar Cells
AIP Conf. Proc. 2367, 020003-1–020003-7; https://doi.org/10.1063/5.0055978
Published by AIP Publishing. 978-0-7354-4101-9/$30.00

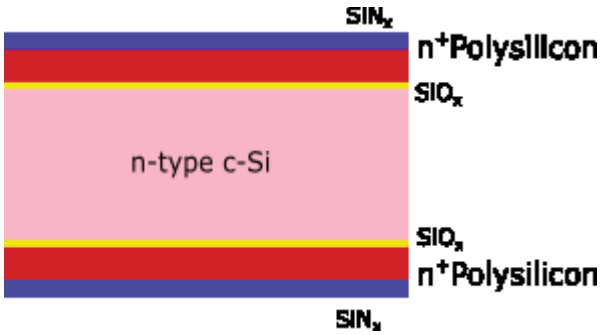

FIGURE 1. A schematic representation of the sample used in the work.

Implied open-circuit voltage (iV_{oc}) and minority charge carrier lifetime measurements were performed using a QSSPC Sinton WCT-120 lifetime tester [6]. The measurements were carried out in the center region of the samples. This was done because the center region as marked in Fig. 2a as MF1 remains unmetallised throughout the process. Samples were metallised by screen printing with three different pastes, marked in the following as Paste A, B and C. The three pastes were supplied by a major paste manufacturer, specially designed for application with polysilicon layers. After metallisation, another QSSPC measurement was carried out and the Photoluminescence (PL) images were recorded. Based on the QSSPC results, the PL images were converted into iV_{oc} calibrated images. From these the recombination current density (J_{01}) is calculated using the single diode model, which is then plotted as a function of metal fraction, as shown in Fig. 2c. Finally, the J_{0met} is extracted from the linear fit of this data [7]. Contact resistivity was measured using Transmission Line Measurement (TLM) method. We only measure an effective contact resistivity containing potentially contributions between metal paste and polysilicon layer and to a smaller extent between polysilicon layer and bulk wafer. We do not aim to decompose these components in this work. We assume that the main contribution stems from metal paste to polysilicon layer.

Furthermore, we took Scanning Electron Microscope (SEM) images to visualize and understand the interaction between silver paste and the polysilicon layer. Three-step chemical etch back of silver and glass frit was used to prepare the samples for SEM, as shown in Fig. 3. After each step, SEM images were recorded and compared with corresponding images for the other pastes.

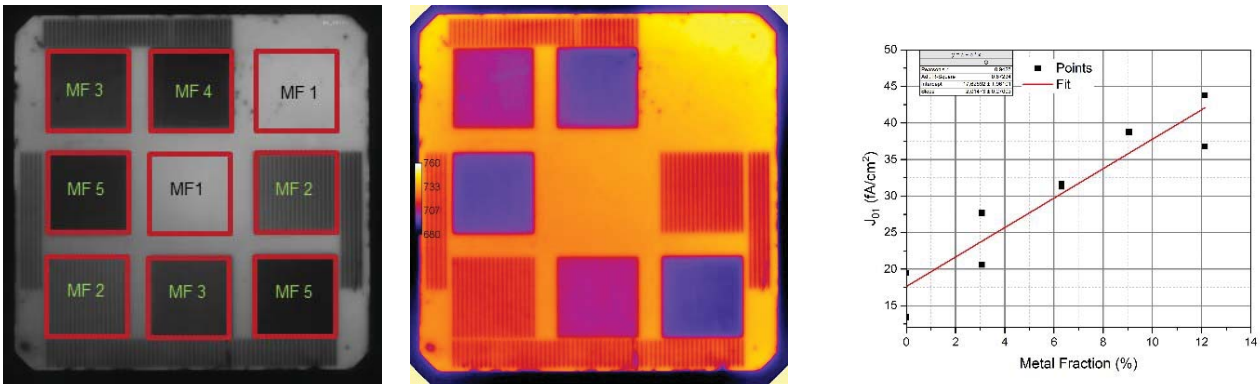

PL Images iV_{oc} Calibrated Image J_{01} vs. Metal Fraction (MF) (%)

FIGURE 2. (a) An example of the PL image, in which patches with different density of metal lines are marked by red squares as MF1 to MF5, (b) Implied voltage calibrated PL image and (c) plot of J_{01} as a function of metal fraction of the spots marked in the PL picture. J_{0met} is extracted from the slope of the regression line. This sample in this figure is used as an example to explain how the J_{0met} is extracted.

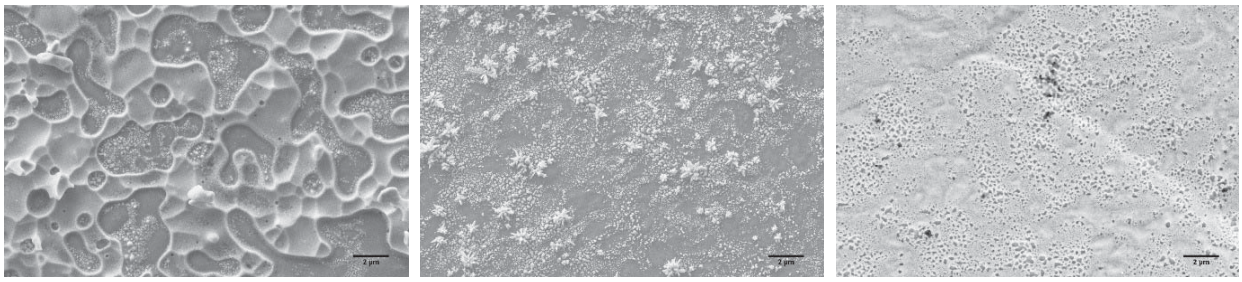

(a)	(b)	(c)
Step 1	Step 2	Step 3
HNO_3 Dip	HF Dip	HNO_3 Dip
Bulk Silver Removal	Glass layer removal	Silver crystallite removal

FIGURE 3. SEM images after different chemical treatments to remove (a) Bulk Silver (b) Glass layer and (c) Silver crystallites in Step 1, 2 and 3. The sample shown here was printed using Paste A and fast fired at peak temperature of 820°C.

RESULTS AND DISCUSSION

The passivation quality of the samples in the non-metallized area was determined with the QSSPC measurements. The results are presented in Fig. 4. A good level of passivation is obtained for the samples, both directly after SiN_x deposition and after fast firing in a belt furnace, with mean iV_{oc} above 720 mV and mean half J_{01} below 9 fA/cm^2.

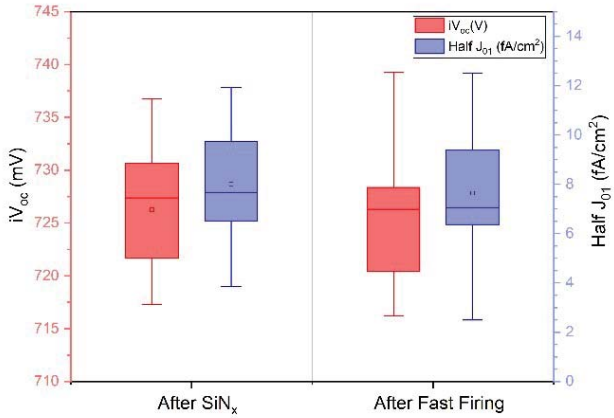

FIGURE 4. Implied open circuit voltage (iV_{oc}) and surface recombination current density (J_{01}) of the samples in the non-metallised part.

Looking at the PL images presented in Fig. 5, we can see a transition from dark metallised squares (which translates to higher recombination as compared to the unmetallised squares) at a fast firing peak temperature of 820 ^{0}C to brighter squares at 790 ^{0}C for the three different pastes. The fast firing peak temperature is the set fast firing temperature in the highest temperature zone of the fast firing furnace. For Paste A and B, at 790°C almost no reduction of the PL signal due to metallization is visible, whereas for Paste C also at 790°C a certain reduction of the PL signal remains. Vanishing visibility of the metal print means that the contribution from the metal polysilicon recombination is not significant in comparison to the surface recombination.

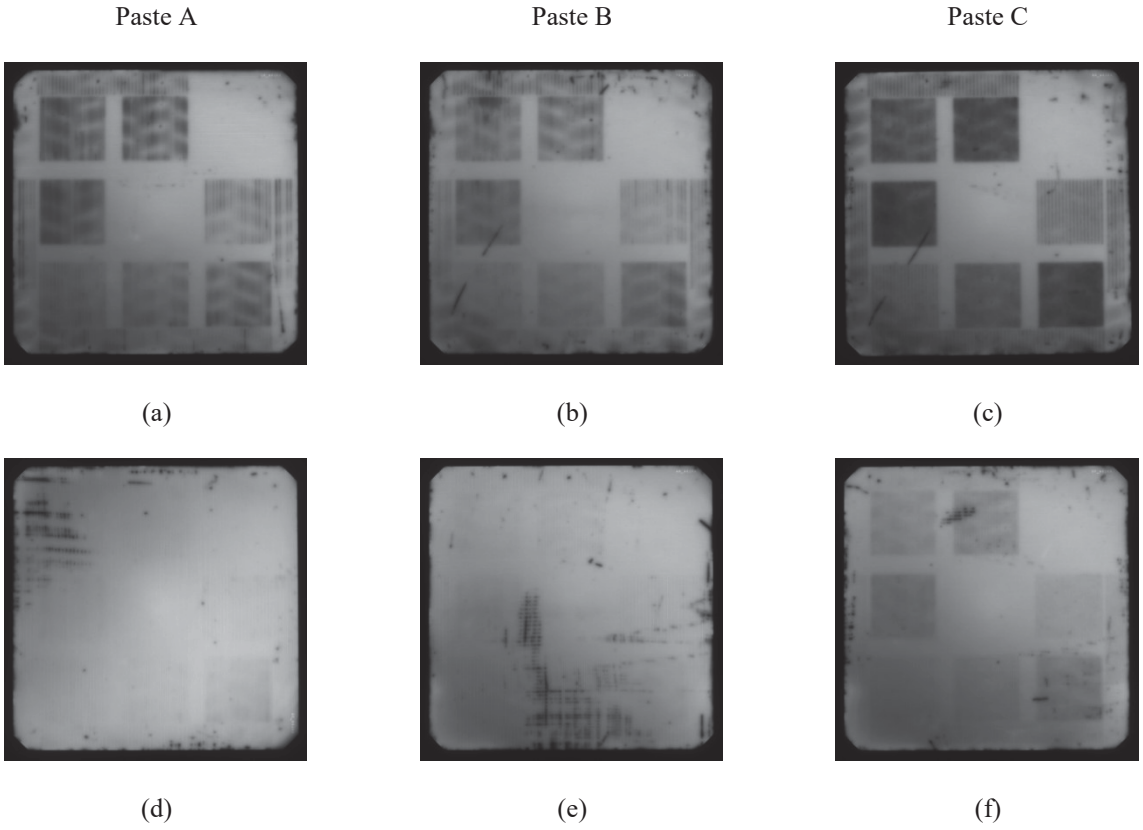

FIGURE 5. PL images of the samples: (a), (b) and (c) are fired at 820^0C, (d), (e) and (f) are fired at 790^0C. (a) and (d) are printed using Paste A , (b) and (c) with Paste B, and (c) and (f) with Paste C. All the PL images were taken at the same optical parameters (illumination, aperture and integration time). Irregular black features like in the upper left corner of picture (d) are believed to be due to scratches. Squared black area, like in picture (c) are due to metal recombination.

In a same way, pictures were recorded for the full fast firing peak temperature range from 760 ^{0}C to 820 ^{0}C, with steps of 15 ^{0}C. J_{0met} values were computed from the pictures as described above. Fig. 6 shows the J_{0met} obtained at different fast firing peak temperature for the three pastes. For vanishing metal recombination, it is not possible to calculate a J_{0met} value from the PL picture. In these cases we set an upper limit of 70 fA/cm^2. This was the value of the last PL picture which allowed reliable determination of J_{0met}, Paste A fired at 820°C. We verified by direct comparison, that all remaining PL images showed lower contrast as this picture; hence metal recombination for these must be lower than 70 fA/cm^2. Fig. 6 shows that when the fast firing peak temperature is increased the J_{0met} increases, at least above a certain threshold. This is consistent with results which we published earlier [7].

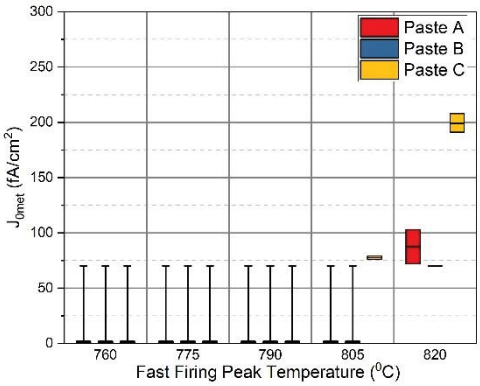

FIGURE 6. J_{0met} for the three pastes at different fast firing peak temperatures.

Of the three pastes, paste C shows higher metal polysilicon recombination as compared to paste A and B.

To understand the decrease in J_{0met} on decreasing the fast firing peak temperature, we also compare the SEM images after the complete etching of the silver paste, glass layer and silver crystallites (step 3 from Fig. 3) as shown in Fig. 7 for the sample printed with Paste A.

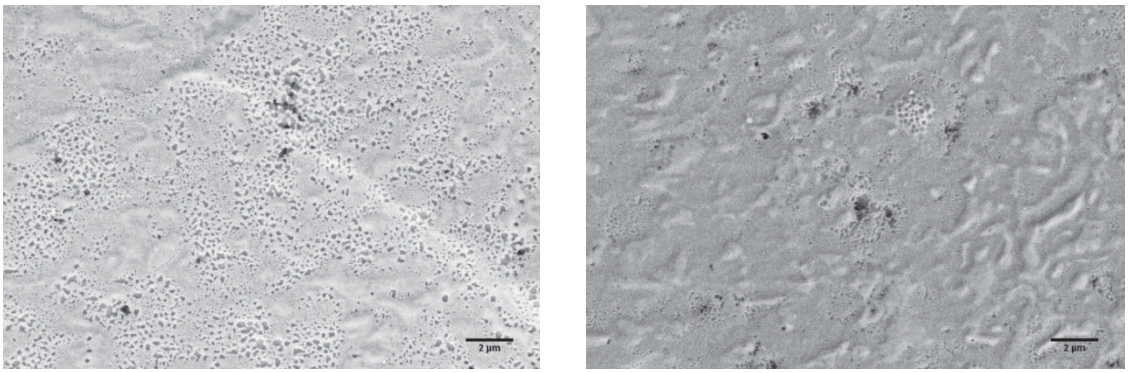

(a) (b)

FIGURE 7. Sample fired with fast firing peak temperature of (a) 820 ^{0}C and (b) 760 ^{0}C.

Looking at the SEM images we can ascertain that the sample fired at higher fast-firing peak temperature has more sites where the polysilicon layer has been removed or damaged (visible as dark valleys and black spots in the images). These are the sites where the silver crystallites might get in contact with the silicon wafer. Such etching of the polysilicon layer has been also observed in literature before [9, 10]. A lower density of sites with damaged and removed polysilicon layer correlates with a low J_{0met}. We also observed the same for the other pastes.

In Fig. 8, the contact resistivity values with respect to the fast firing peak temperature are presented.

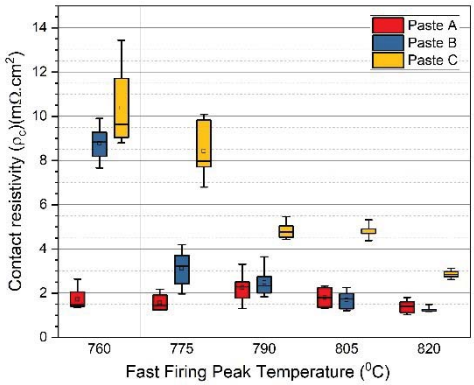

FIGURE 8. Contact resistivity for the three pastes at different fast firing peak temperatures.

For Paste A we don't observe a significant difference in the values at different fast firing peak temperatures. The mean value of contact resistivity remains below 2 mΩ.cm^2 for the fast firing peak temperatures investigated, except at 790 ^{0}C where it is slightly above at 2.2 ± 0.7 mΩ.cm^2. Paste A shows good performance even at a low fast firing peak temperature of 760 ^{0}C. The lowest mean value of 1.4 ± 0.3 mΩ.cm^2 is obtained for Paste A fired at 820 ^{0}C. However, for Paste B and C contact resistivity increases at lower fast firing temperatures. For example for Paste C, the contact resistivity increases from 2.8 ± 0.2 mΩcm^2 at 820 ^{0}C to 10.4 ± 2.1 mΩ.cm^2 at 760 ^{0}C.

From the above contact resistivity results coupled with the low J_{0met}, Paste A would be the favourable paste for contacting a 150 nm insitu doped n^+ polysilicon based passivated contact with a wet chemical thin oxide. It shows low J_{0met} value below 70 fA/cm^2 and contact resistivity below 2 mΩ.cm^2 throughout the investigated fast firing peak temperature range. These values are among the lowest obtained values to the best of our knowledge.

CONCLUSION

We have shown excellent J_{0met} values on 150-nm thick n-type polysilicon passivated contact layer stacks using industrial screen printing processes with a firing-through Ag paste. A fast-firing optimisation was performed by varying the peak temperature of the fast-firing furnace. From this experiment, we were also able to obtain J_{0met} values of 70 fA/cm^2 for the samples fired at peak temperature of 820 ^{0}C. At this temperature the mean effective contact resistivity is as low as 1.4 ± 0.3 mΩ.cm^2 (Paste A). Also the contact resistivity of this paste remains almost low throughout the investigated fast firing peak temperature range. With the low J_{0met} values, Paste A is the favourable paste for metallisation for our layers. We also see from the SEM images that the J_{0met} value is related to the number density of the sites where the polysilicon layer has been removed and damaged.

ACKNOWLEDGMENTS

This work was supported by German Federal Ministry for Economic Affairs and Energy under contract number 0324198A (TuKaN). We would also like to thank Heraeus for supply of the silver pastes and Frank Huster (University of Konstanz) for his support in taking SEM images.

REFERENCES

1. Chen, D., et al. "24.58% total area efficiency of screen-printed, large area industrial siliconsolarcells with the tunnel oxide passivated contacts (i-TOPCon) design." Solar Energy Materials and Solar Cells 206 (2020): 110258.
2. Feldmann, F., et al. "Large area TOPcon cells realized by a PECVD tube process." Proc. 36th Eur. Photovolt. Sol. Energy Conf. Exhib.. 2019.

3. Padhamnath, P., et al. "Characterization of screen printed and fire-through contacts on LPCVD based passivating contacts in monoPoly™ solar cells." Solar Energy 202 (2020): 73-79.
4. Messmer, C., et al. " Upgrade PERC with TOPCon: Efficiency Potential by taking into account the Electrical Gains and Optical Losses." Proc. 36th Eur. Photovolt. Sol. Energy Conf. Exhib.. 2019
5. Messmer, C., et al. "Efficiency Roadmap for Evolutionary Upgrades of PERC Solar Cells by TOPCon: Impact of Parasitic Absorption." IEEE Journal of Photovoltaics 10.2 (2019): 335-342.
6. Sinton, R., et al. (1996, May). Quasi-steady-state photoconductance, a new method for solar cell material and device characterization. In Conference Record of the Twenty Fifth IEEE Photovoltaic Specialists Conference-1996 (pp. 457-460). IEEE
7. Chaudhary A., et al. Screen printed Ag contacts for n-type polysilicon passivated contacts. In: AIP Conference Proceedings, vol. 2147 AIP Publishing; 2019. p. 040002
8. Comparotto, C., et al. “Understanding contact formation on n-PERT-RJ solar cells”. Proceedings of the 33 rd EUPVSEC Conference, Amsterdam, The Netherlands, 2017, pp. 832-836.
9. Stodolny M., et al. “PolySi Based Passivating Contacts Enabling Industrial Silicon Solar Cell Efficiencies up to 24%”. IEEE 46th Photovoltaic Specialists Conference (PVSC). IEEE, 2019.
10. Mack, S., et al. “Metallisation of boron-doped polysilicon layers by screen printed silver pastes”. physica status solidi (RRL)–Rapid Research Letters 2017, 11(12), 1700334.